

Pion femtoscopy in Au+Au collisions at $\sqrt{s_{NN}} = 3$ GeV in the STAR experiment

Anna Kraeva (for the STAR Collaboration)^{1,*}

¹*National Research Nuclear University MEPhI*

There is a method, called femtoscopy, that allows us to measure directly the spatio-temporal extent of the region where particles are emitted and the parameters of the nuclear-nuclear interaction. In heavy-ion collisions, femtoscopy is an important tool for studying the geometric and dynamic characteristics of the particle emission region. Two-particle momentum correlations of identical particles in nuclear-nuclear collisions make possible to extract femtoscopic parameters (radii of emission region, R , and correlation strength, λ). Reaction dynamics is reflected in the femtoscopic radii dependence on pair transverse momentum, k_T . This work is devoted to the study of two-particle momentum correlations of identical pions produced in collisions of gold nuclei at $\sqrt{s_{NN}} = 3$ GeV in the STAR experiment at RHIC. The extracted three-dimensional femtoscopic radii (R_{out} , R_{side} , R_{long}) are measured as a function of k_T for 0-10% central Au+Au collisions.

I. INTRODUCTION

The method of correlation femtoscopy allows one to measure the spatial extent of particle emission and the parameters of the hadron-hadron interaction. This method was developed in elementary particle physics where an increase in the number of like-sign pion pairs with respect to unlike-sign pion pairs was found at small relative angles between pions [1–4]. Quantum statistics effects of this kind are explained by the following property of the resulting particles: identical boson pairs (particles with an integer spin), obeying the Bose-Einstein statistics, are more probable to be detected in a close region of the phase space.

This work is devoted to the study of two-particle momentum correlations of identical pions in the STAR experiment at RHIC, the size of the emission region of identical pions is

* annakraeva555@gmail.com

27 studied and estimated by constructing the correlation functions.

28 II. ANALYSIS METHOD

29 The task of correlation femtoscopy is to obtain a certain function from the available
30 experimental data, which characterizes the source of emission of particles in the process of
31 collision of nuclei or elementary particles. This method makes possible to estimate the size
32 of the source and the time of particle emission.

33 The experimental correlation function represents the ratio of the distribution, $A(\vec{q})$, of the
34 relative momenta of pairs of identical particles, $\vec{q} = \vec{p}_1 - \vec{p}_2$, from one event to the analogous
35 reference distribution, $B(\vec{q})$, where quantum-statistical correlations are absent [5]:

$$36 \quad C(\vec{q}) = \frac{A(\vec{q})}{B(\vec{q})}. \quad (1)$$

37 In the study of two-particle correlations, the choice of a reference distribution plays an
38 important role. The reference distribution is constructed according to the same selection cri-
39 teria for single particles except for the presence of quantum-statistical correlations, Coulomb
40 effects, and strong final state interactions. One of the methods for making the reference
41 distribution is the event-mixing technique, in which each particle from a pair of particles
42 belongs to different events. Thus, all the experimental effects like detector acceptance are
43 reproduced without physics correlations between the two particles, such as Bose-Einstein
44 correlation and final state interactions.

45 The relative momentum, \vec{q} , contains three independent components ($q_{out}, q_{side}, q_{long}$),
46 while the source is described by three spatial and one temporal dimensions. As a result, the
47 relative momentum components are expressed in terms of a certain set of correlation radii,
48 depending on the choice of reference system and parameterization.

49 The most widely used "Out-Side-Long" parameterization is defined as follows [6, 7]. The
50 coordinate system in the space of relative momentum $\vec{q} = \vec{p}_1 - \vec{p}_2$ of a pair of particles is
51 chosen so that the *long* direction is parallel to the beam axis, the direction *out* is parallel
52 to the direction of the total transverse momentum of the pair $\vec{k}_T = (\vec{p}_{1,T} + \vec{p}_{2,T})/2$, and the
53 *side* direction is perpendicular to the long and out directions.

54 In this work, Longitudinally Co-Moving System (LCMS) [8], where $p_{1,z} + p_{2,z} = 0$, was
55 used. The $p_{1,z}$ and $p_{2,z}$ are the projections of the momenta of the first and second particles

56 onto the z axis.

57 The radii of the particle emission region are known to depend on k_T for an expanding
58 source. In the LCMS system, the correlation function can be represented as the Bowler-
59 Sinyukov function [9, 10]:

$$60 \quad C(q) = N[(1 - \lambda) + \lambda K(q)(1 + G(q))], \quad (2)$$

61 where λ is the coefficient characterizing the strength of femtosopic correlations, $K(q)$ is the
62 Coulomb factor describing the Coulomb repulsion in the case of identical particles, N is the
63 normalization factor. The term $G(q)$ represents the Gaussian source function and can be
64 described by the following equation:

$$65 \quad G(q) = \exp(-q_o^2 R_o^2 - q_s^2 R_s^2 - q_l^2 R_l^2 - 2q_o q_s R_{os}^2 - 2q_s q_l R_{sl}^2 - 2q_o q_l R_{ol}^2), \quad (3)$$

66 where R_i and R_{ij} are the components of femtosopic radii, where $i, j = \{out, side, long\}$.
67 In this work, the cross components of the radii of the emission region (R_{os}, R_{sl}, R_{ol}) were
68 considered to be negligible.

69 Experimental correlation functions are usually fitted by Eq. 2. The extracted radii do
70 not determine the size of the entire source, but the size of the "homogeneity" region [11],
71 which is a part of the source region that emits particles with similar momenta.

72 III. EXPERIMENT AND EVENT, TRACK, PARTICLE AND PAIR 73 SELECTIONS

74 The data used for the analysis were obtained in the STAR experiment at RHIC [12]. The
75 minimum bias Au+Au collisions at $\sqrt{s_{NN}} = 3$ GeV were analyzed. The beam was incident
76 on a gold target 0.25 mm thick corresponding to a 1% interaction probability. The target is
77 installed in a vacuum pipe at 200.7 cm west of the STAR center and 2 cm below the beam
78 axis [13].

79 Events reconstructed within $195 < V_Z < 205$ cm and $V_R = \sqrt{V_X^2 + V_Y^2} < 2$ cm were
80 used in the analysis. V_z is the vertex position along the beam direction and V_R is the radial
81 vertex position.

82 One of the characteristics of nuclear collisions is multiplicity. For the Fixed-target pro-
83 gram (FXT), the multiplicity is defined as the number of reconstructed primary particles

(particles fitted to the reconstructed collision vertex). The values of the obtained multiplic-
 ity are compared with the ranges of centralities that characterize the degree of overlap of two
 nuclei during a collision. Only events that correspond to 0-10% central Au+Au collisions
 were analysed in this study.

Tracks with more than 15 ionization points inside the Time Projection Chamber (TPC) [14],
 distance of closest approach (DCA) $DCA < 3$ cm and pseudorapidity $-2 < \eta < 0$ were
 used in the analysis. Pion identification was performed by the combination of ionization
 energy loss in TPC and velocity measured in the Time-Of-Flight detector (TOF) [15]. At
 low particle momentum ($0.15 < p < 0.55$ GeV/c) the method of identification using TPC
 was done by measuring the ionization energy losses of charged particles dE/dx for each track
 and comparing it to the expected value for each particle type i using the dE/dx resolution:

$$n\sigma_i = \frac{1}{\sigma_i} \log \left(\frac{dE/dx_{measured}}{dE/dx_{expected,i}} \right). \quad (4)$$

The following criteria were required for pion identification: $|n\sigma(\pi)| < 2$ and
 $|n\sigma(e, K, p)| > 2$, which suppresses contamination from other particles.

At $0.55 < p < 1.5$ GeV/c, the $|n\sigma(\pi)| < 3$ was required for the ionization energy loss in
 TPC and $-0.05 < m^2 < 0.08$ GeV²/c⁴, $|1/\beta - 1/\beta(\pi)| < 0.015$ were required using the
 information from TOF, where β is the particle velocity. The momentum range selected is
 based on the fact that pions are clearly separable from electrons, kaons, and protons. The
 purity of pions is not lower than 99%.

Due to the imperfection of track reconstruction, the effects of track merging (two tracks
 reconstructed as one) and track splitting (one track reconstructed as two) may occur and
 distort correlation function [5]. The Fraction of Merged Hits (FMH) is estimated as the ratio
 of the number of merged hits to the maximum possible number of hits for the reconstruction
 of the track - 45. The Splitting Level (SL) is estimated as:

$$SL = \frac{\sum_{i=1} S_i}{Nhits_1 + Nhits_2}, \quad (5)$$

where $S_i = +1$ if only one track from the pair has a hit, $S_i = -1$ if both tracks from the
 pair have hits, $S_i = 0$ if none of the tracks has no hit in the detector plane. $Nhits_1 + Nhits_2$
 is the sum of the number of hits of the two tracks.

112 To minimize those effects, only pairs that pass two-track selection criteria were used in
 113 the analysis: splitting level required to be in a range $-0.5 < SL < 0.6$ and fraction of
 114 merged hits should be in a range $-1.1 < FMH < 0.1$.

115 To study the dynamics of the particle production, femtoscopic analysis was performed in
 116 4 regions of k_T : $[0.15, 0.25]$, $[0.25, 0.35]$, $[0.35, 0.45]$, $[0.45, 0.55]$ GeV/ c .

117

IV. RESULTS

118 The correlation functions were constructed in the centrality range 0–10% of most central
 119 collisions. Correlation functions of positive and negative pion pairs were studied separately.
 120 Figure 1 shows the correlation functions of positively (grey markers) and negatively (black
 121 markers) charged pions projected into out (left), side (middle), and long (right) directions
 122 with $0.15 < k_T < 0.25$ GeV/ c .

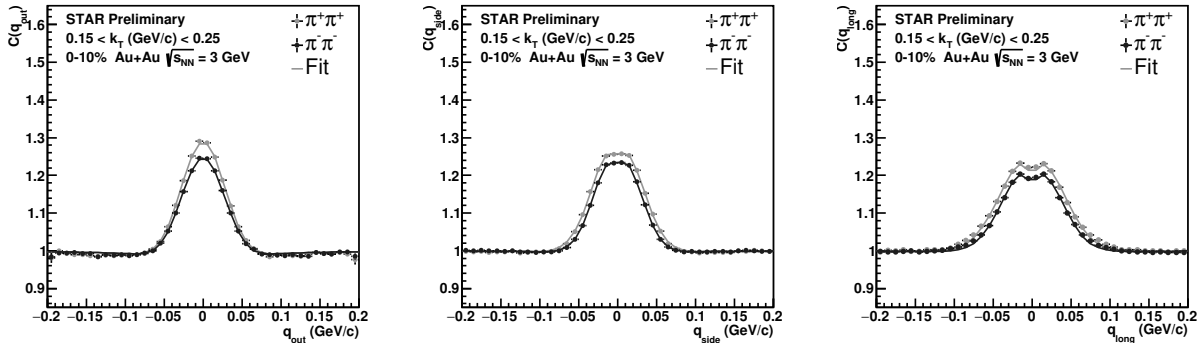


FIG. 1. Correlation functions of positive (grey markers) and negative (black markers) pions with a centrality of 0-10% in the range $0.15 < k_T < 0.25$ GeV/ c at $\sqrt{s_{NN}} = 3$ GeV in Au+Au collisions. In each case the other components are projected over ± 0.05 GeV/ c

123 The parameters of the particle emission region (the radii of the emission region
 124 R_{out} , R_{side} , R_{long}) extracted by fitting the correlation functions were plotted depending
 125 on the ranges of the k_T in Fig. 2. The values of k_T for positive pions are shifted for clarity.

126 The systematic uncertainties in the extracted radii were estimated based on the variation
 127 of pair cuts applied. Also, the Coulomb correction factor $K(q)$ and fitting range were varied.
 128 The contribution to the systematic uncertainties is about 4% for the FMH cuts, 0.02% for
 129 the SL cuts, 0.1% for the fit range, 1.5% for the $K(q)$.

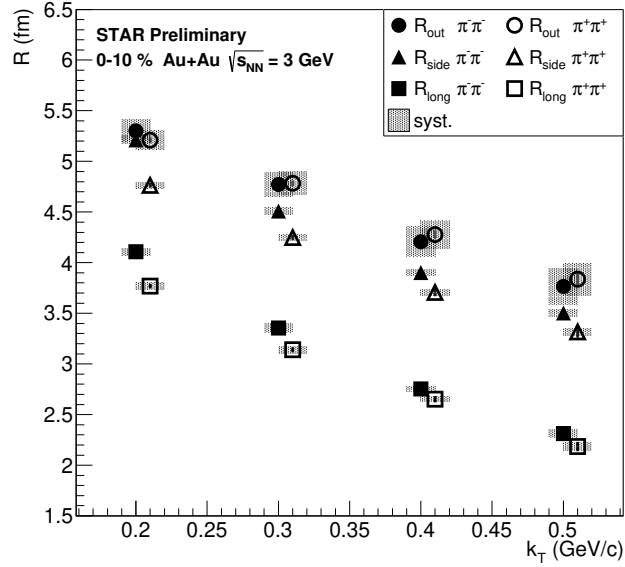


FIG. 2. Extracted pion source radii (R_{out} , R_{side} , R_{long}) as a function of the k_T for the centrality range 0-10% in Au+Au collisions at $\sqrt{s_{NN}} = 3$ GeV

130 Femtoscopic radii decrease with increasing k_T due to a decrease in the emission region of
 131 the system due to transverse flow. Correlation functions of positive and negative pions differ
 132 slightly for small k_T , which may be due to mean field interaction [16]. The values of the
 133 radii are slightly smaller than for higher energies, which is associated with a shorter system
 134 lifetime.

V. SUMMARY

135
 136 In this work, correlations of identical pions produced in collisions of gold nuclei at
 137 $\sqrt{s_{NN}} = 3$ GeV have been studied. The three-dimensional correlation functions of positive
 138 and negative pions were studied in 4 ranges of the k_T in 0-10% centrality and fitted
 139 with the Bowler-Sinyukov function. The extracted femtoscopic radii decrease with increasing
 140 k_T due to a decrease of the system size in the emission region due to transverse flow.

141

ACKNOWLEDGMENTS

142 The reported study was funded by the MEPHI Program Priority 2030. The work was
143 partially performed using resources of the heterogeneous computing platform HybriLIT of
144 JINR (LIT) (<http://hlit.jinr.ru>) and NRNU MEPHI high-performance computing center.

-
- 145 [1] G. Goldhaber *et al.*, Phys. Rev. Lett. **3**, 181 (1959)
146 [2] G. Goldhaber *et al.*, Phys. Rev. Lett. **120**, 300 (1960)
147 [3] G. Kopylov, M. Podgoretsky, Sov. J. Nucl. Phys. **15**, 219 (1972)
148 [4] G. Kopylov, M. Podgoretsky, Sov. J. Nucl. Phys. **18**, 336 (1973)
149 [5] J. Adams *et al.*, Phys. Rev. C. **71**, 044906 (2005)
150 [6] G. Bertsch Nucl. Phys. A. **489**, 6 (1989)
151 [7] S. Pratt Phys. Rev. Lett. **53**, 1219 (1984)
152 [8] M. Lisa *et al.*, Ann. Rev. Nucl. Part. Sci. **55**, 357 (2005)
153 [9] M. Bowler, Z. Phys. C. **39**, 81 (1988)
154 [10] Yu. Sinyukov *et al.*, Phys. Lett. B. **432**, 248 (1998)
155 [11] S. Akkelin, Yu. Sinyukov, Phys. Lett. B. **356**, 525 (1995)
156 [12] K. Ackermann *et al.*, Nucl. Instrum. Meth. A. **499**, 624 (2003)
157 [13] J. Adam *et al.*, Phys. Rev. C. **103**, 3 (2021)
158 [14] M. Anderson *et al.*, Nucl. Instrum. Meth. A. **499**, 659 (2003)
159 [15] W. Llope *et al.*, Nucl. Instrum. Meth. A. **522**, 252 (2004)
160 [16] J. Barrette *et al.*, Phys. Rev. C. **55**, 1420 (1997)